IRSTI 44.09.29

Self-regulated hydrogen generation with the use of nano-powders: application for portable fuel cells

A. Pastushenko[1,#], S. Litvinenko[1], V. Lysenko[2,*] and V. Skryshevsky[1]

[1]*Institute of High Technologies, National Taras Shevchenko University of Kyiv,
Volodymyrs'ka 64, Kyiv 01601, Ukraine*
[2]*Lyon Institute of Nanotechnologies (INL), CNRS UMR-5270, INSA de Lyon,
7 av. Jean Capelle, Bat. Blaise Pascal, Villeurbanne, F-69621, France*
[#]*Current affiliation: Apollon Solar SAS, 66 Course Charlemagne, 69002 Lyon, France*
[*]*e-mail: vladimir.lysenko@insa-lyon.fr*

Self-regulated hydrogen production at room temperature and atmosphere pressure is described in details. Basic idea of our approach is based on a precise auto-tuning of the oxidizing aqueous solution arrival onto hydrogenated silicon or aluminum nano-powders. The used self-regulation principle is completely passive e.g. neither electrical power sources, no regulating electronics are required. The system functioning was simulated numerically and checked experimentally. The numerical simulation allowed definition of the main optimal parameters of the working system (pressure, capillary tube diameter, tank volumes) and an experimental prototype based on the simulated results was built and used for hydrogen supplying to a portable PaxiTech® fuel cell.

Key words: hydrogen generation, nano-powders, fuel cells.
PACS numbers: 81.05.Rm, 81.07.Wx, 88.30.-k.

1 Introduction

Hydrogen energy field is rapidly developing, presenting hydrogen as a new friendly-environmental energy carrier. However, to ensure wide usage of hydrogen, energy density of new hydrogen-based energy sources have to exceed the value of 180-200 W·h/kg which is the maximal level for traditional power sources such based on lithium-ion batteries. Thus, elaboration of new efficient ways for hydrogen production and storage is of the highest importance.

Traditional hydrogen storage in high pressure vessels is not applicable for small portable devices due to safety reasons. One of the alternative ways is storing hydrogen in capillary arrays [1, 2]. However, leakage of H_2 through thin capillary walls is the main disadvantage of this technological approach. Another solution to store hydrogen is the use of zeolites [3] with hydrogen mass content 1-2 % at 77 K and 1.6 MPa. Metal hydrides [4] seem to be also perspective candidates for portable and reversible hydrogen storage with relatively high mass content up to 7.6%. However, quite high temperatures are required for hydrogen desorption. In addition,

desorption kinetics should be faster and there should be more number of cycles. Hydrolysis of metal hydrides overcomes some of these problems, but it is not reversible. Application of the hydrolysis for large automotive devices have been reported [5]. Hydrogen generation by solid Co-P catalyst from water solution of NH_3BH_3 have been also discribed [6]. The solid catalyst is quite attractive because of its constant H_2 production rate.

Hydrogen generation based on corrosion of light metals in water solutions is an interesting alternative for hydrogen sources. In particular, Al is probably the most adequate metal due to its high electron density and oxidation potential. However, the problem related to passivation of Al due to formation of $Al(OH)_3$ inhibiting H_2 formation remains unsolved. Thus, for generation of H_2 from water, using of Al powder and alkaline solutions are rather needed [7].

Porous silicon (PS) nanostructures can be conceived as solid-state hydrogen reservoir since its specific surface is almost totally covered by $Si-H_X$ bonds [8-18]. Theoretical maximum of the hydrogen content is 3.44 mass% for SiH, 6.66 mass% for SiH_2 and 9.67 mass% for SiH_3 species [13]. Maximal

quantity of hydrogen extracted from this kind of nanomaterials due to thermal annealing is about 60 mmol(H) per gram of PS (~6 mass%). This corresponds to about 1.8 of the H/Si ratio [9]. H_2 can be also produced from the PS at room temperature due to its oxidation in aqueous solutions. Thus, practical H_2 output resulted from the reaction with water is 2-3 times larger because water dissociation also provides two additional molecules of hydrogen [8].

A bottleneck in practical applications of portable fuel cells is perfectly controllable extraction of hydrogen from a tanker. While a portable device is switched on and consumes electrical power from a fuel cell, hydrogen must be generated in a reactor chamber. The evolution of hydrogen must be automatically stopped after the electrical consumer switching off. For example, a self-regulating hydrogen generator for micro fuel cells was earlier conceived [20]. The device consists of a hydride reactor and a water reservoir separated by a regulating valve. The latter is connected to the water reservoir and contains a movable membrane with holes. Water diffuses toward the hydride reactor due to capillary forces in the pores of the membrane. After reduction of hydrogen consumption, the gas pressure builds up inside the hydride reactor and provokes deflection of the membrane closing the water regulator valve. Maximum electrical power delivered by this device was measured to be 2.4 mW/cm^2 (8 mA/cm^2 at 0.3 V). However, the maximum limit power of a PEM fuel cell is about 210 mW/cm^2 (700 mA/cm^2 at 0.3 V). Comparing the systames described in Refs. [20] and [5], one can see a huge difference in power values. In Ref. [5], the authors work with water flows and control it electronically. In Ref. [20], the water vapors generate small power and any electrical control would dramatically decrease the total efficiency of the hydrogen generator.

In this paper, to control hydrogen production with the use of Al or PS nanopowders, a drop-by-drop approach based on an original double-tank hydrogen cartridge is described. For this approach, no active electrical control is necessary due to a self-regulating mechanism. Our cartridge can automatically stop production of hydrogen when it is not consumed by a fuel cell. The first tank of the cartridge contains a liquid oxidizer and the second one – PS or Al nanopowder. The tanks are connected via a capillary tube. The self-regulation mechanism is realized due to the dynamical variation of pressure difference between the tanks. If the pressure difference exceeds capillary pressure, a drop of the liquid oxidizing reagent falls down from the first to the second tank and reacts with the nanopowder. It leads to increase of the hydrogen pressure in the second chamber and, thus, decreasing the pressure difference. If the pressure difference is less than the capillary pressure, no oxidizer falls down and the system is in a stand-by state and waits for the hydrogen consumption by a fuel cell to decrease the hydrogen pressure in the second tank and, consequently, to increase the pressure difference. Numerical analysis of the cartridge functioning was performed and optimal parameters have been found. A working prototype of the cartridge was constructed and tested with a PaxiTech® fuel cell.

2 Double-tank cartridge for hydrogen supply

To ensure a self-regulating hydrogen production, a principle of on-demand supplying of reactants can be applied. A scheme of our hydrogen cartridge is shown in Figure 1. The cartridge consists of two tanks interconnected with a capillary tube. An upper tank contains pressurized air chamber at pressure p_1 slightly higher then the atmospheric pressure. The reaction between an oxidizer and PS or Al nanopowders takes place in the lower tank in which the generated hydrogen ensures a pressure value p_2. Diameter of the capillary tube should be small enough to ensure capillary phenomena as well as to maintain an equilibrium when pressure difference ($p_1 - p_2$) between the both tanks is less than the capillary pressure. Thus, it is possible to stop dropping when the final pressure difference due to the hydrogen generation becomes less than the capillary pressure and this is achieved without using of any valve. This is the first major advantage of our cartridge. Using of the capillary forces allows establishing of much more precise hydrogen generation rates compared to the use of valves and continuous water flows.
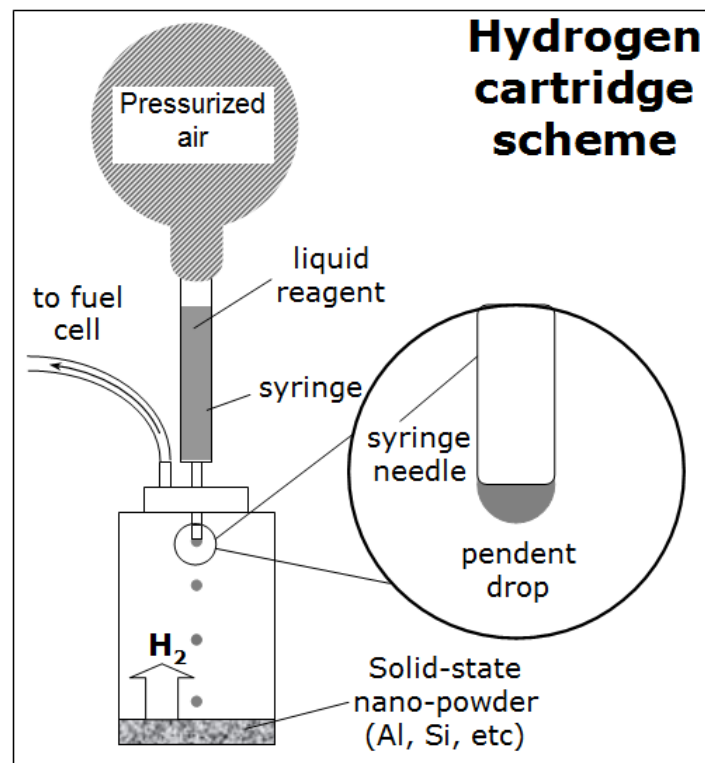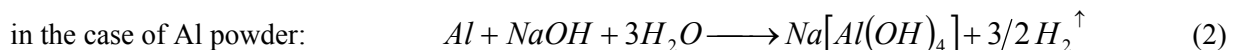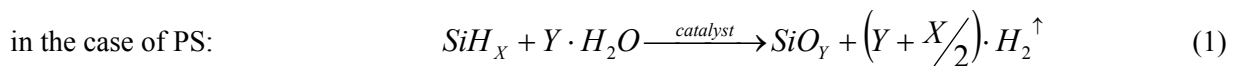
Figure 1 - Scheme of the double-tank cartridge for hydrogen generation
with the use of Al or PS nanopowders

The first oxidizing reactant (water/catalyst or liquid alkaline solution) is spatially separated from another reactant (solid-state PS or Al nanopowder). Reaction chamber (lower tank with powder) has hydrogen outlet which is connected to a fuel cell. The corresponding chemical reactions between the water-based oxidizers and nanopowders are the follows:

in the case of PS:

$$SiH_X + Y \cdot H_2O \xrightarrow{catalyst} SiO_Y + \left(Y + \frac{X}{2}\right) \cdot H_2^{\uparrow} \qquad (1)$$

in the case of Al powder:

$$Al + NaOH + 3H_2O \longrightarrow Na[Al(OH)_4] + 3/2\,H_2^{\uparrow} \qquad (2)$$

Let's calculate the maximum possible gravimetric energy density for the reactions (1) and (2). In the reaction (1), we assume X=2, Y=2, which correspond to the case of fresh and completely hydrogenated nano-porous silicon. The product of the reaction (1) is silica gel keeping physically absorbed water. Let's assume that 1 mol of SiO_2 keeps 1.5 mol of water. Thus, 1 mol of SiH_2 (30 g) needs 3.5 mol of water (63 g), and it gives 3 mol of hydrogen. Mass of the used catalyst (NH_3, for example) comes in trace quantities which can be neglected [8]. Assuming that efficiency of a standard PEM fuel cell is about 50 % [21], electrical energy value which can be obtained from such reaction is 99 W·h. Thus, the corresponding gravimetric energy density is 99 W·h/(30g+63g) = 1054 W·h/kg, which is motre than 5 times larger than the energy density provided by traditional Li-ion batteries.

For the reaction with aluminum powder (2), we obtain: 1 mol of Al (27 g) reacts with 3 mol of water (54 g) and 1 mol of NaOH (40 g), and it gives 1.5 mol of hydrogen. Thus, corresponding electrical energy value is 49 W·h, and the maximum energy density is: 49 W·h/(27g+54g+40g) = 405 W·h/kg.

3 Theoretical description

Now, functional behavior of our hydrogen cartridge will be theoretically described. First of all, let the pressure difference p_1-p_2 between the two tanks be larger than the capillary pressure. Due to the pressure difference, the volume of the drop at the capillary edge starts to increase. The oxidizer flows through a constant circular cross-section of the capillary with a length, which is substantially longer than the capillary diameter. Kinetics of the drop growth can be described by Poiseuille formula [22] which is valid for the laminar, viscous and incompressible flows:

$$\frac{dV_d}{dt} = \frac{\pi r^4}{8\eta l}\left(p_1 - \frac{2\alpha}{r}Cos\theta - p_2 \right), \quad (3)$$

where: V_d is the drop volume, η is the viscosity of the liquid, l is the capillary length, θ is the wetting angle (see Figure 2).
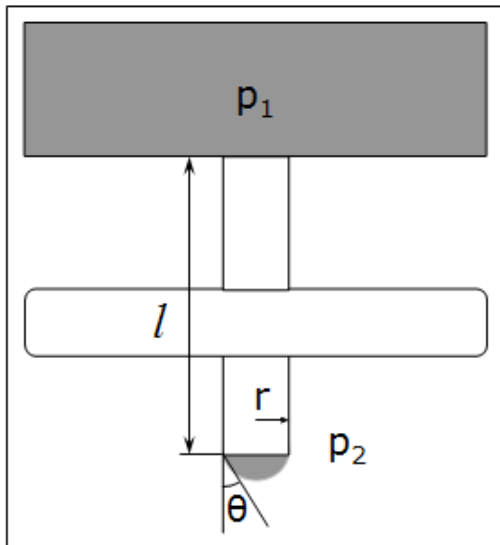

Figure 2 – Characteristical parameters of the cartridge system

The drop falls down when the capillary tension can not compensate the weight of the drop and the pressure difference. The volume of the fallen drop V_d^{max} can be calculated from the following expression:

$$g\rho V_d^{max} = \alpha 2\pi r \quad (4)$$

where: g is the gravitation constant, ρ is the density of the liquid, α is the coefficient of capillary tension and r is the capillary radius.

The total volume of the water in the reaction chamber V_w relates to the number N of hydrogen molecules produced per unit of time:

$$\frac{dN}{dt} = k_r V_w \quad (5)$$

where k_r is the reaction velocity defined as the number of hydrogen molecules produced per unit of time and per unit of water volume. This expression can be applied if the water volume is significantly less than volume of another reactant (nanopowder, in our case). Reaction velocity depends on the temperature, concentration of the catalyst or alkali, and size of powder particles.

Due to the oxidizer consumption, decrease of its volume corresponds directly to the increase of the hydrogen molecules according t the following relation:

$$dV_w = \frac{\mu}{nN_A\rho}dN \quad (6)$$

where: N_A is the Avogadro constant, μ is the oxidizer's molar mass, n is the stoichiometric relation between the oxidizer and hydrogen.

The equations written above can be solved numerically. Thus, pressure of hydrogen in the reaction chamber can be calculated as a function of time. Optimal capillary radius and reaction chamber volume were determined from the numerical calculations.

4 Simulation results

Functioning behavior of the cartridge system has been simulated with the use of the theoretical considerations described above. Two working modes can be defined: (i) steady state mode (Figure 3a) and (ii) dynamic mode (Figure 3b). The steady state mode can be realized with certain cartridge parameters and in absence of hydrogen consumption. In this functioning mode (when the output valve is closed), hydrogen pressure in the reaction chamber increases up to a saturation level which can be kept for a long time. It means that reaction is fully completed and there is no water

supplying into the reaction chamber. As for the dynamic mode, it is realized when the hydrogen output is opened. It is characterized by periodic drop fallings. In this case, the reaction is supported by new falling drops and hydrogen is generated continuously.
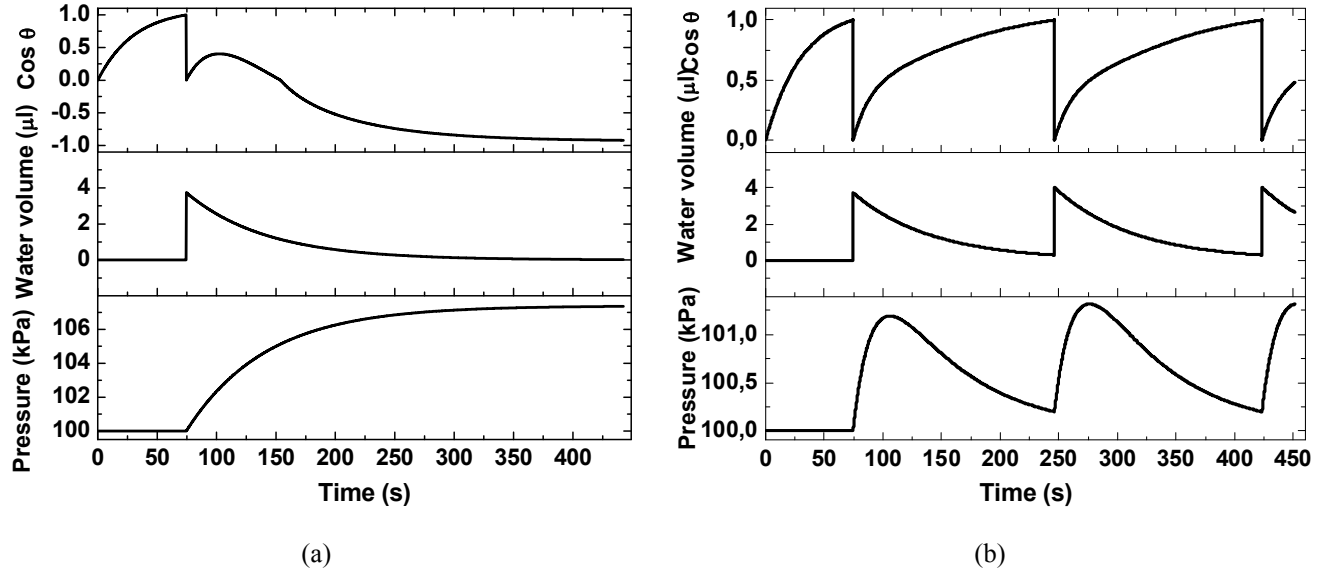

Figure 3 - (a) Steady state and (b) dynamic modes
of hydrogen generation in the cartridge system

The simulation was carried out at $p_1=104$ *kPa*. At the beginning, p_2 was assumed to be equal to 100 kPa. The difference of 4 kPa is slightly larger than the capillary pressure (3600 Pa):

$$\frac{2\alpha}{r} = \frac{2 \cdot 72 \, ^{mN}/_{m}}{40 \mu m} = 3600 Pa \qquad (7)$$

At these initial conditions the first drop can fall. For this simulation, the capillary tension of water and the capillary radius were used to be 72 mN/m and 40 μm, respectively. After the first drop falling, the pressure difference p_1-p_2 decreases due to the production of hydrogen. It should be smaller than capillary pressure to achieve a steady-state mode. Taking into account that the drop volume increases according to the evolved hydrogen pressure, and the hydrogen evolution has exponential character, this problem can not be solved analytically due to the transcendental equation. Thus, a numerical solution has been found. The cosine of the wetting angle was calculated as:

$$Cos\theta = \frac{V_d}{V_d^{\max}} \qquad (8)$$

As one can see in figure 3a, the cosine of wetting angle increases until falling of the first drop. After, the cosine becomes equal to zero and continues to increase. The water volume kinetics in the reaction chamber is also shown in Figure 3a. Before the drop falling, the water volume in the second chamber is equal to zero. Right after the drop falling, the water volume is equal to the drop volume. Due to the water consumption during the chemical reaction of the nanopowder oxidation, the water volume in the reaction chamber progressively decreases to zero. The water vapor is neglected in this simulation. Generation of hydrogen leads to the increase of pressure in the reaction chamber. In our case, the pressure in the reaction chamber increases up to a level which is larger than the pressure in the chamber with pressurized air (104 kPa). As a result, the drop is pushed back in the needle and a bubble is formed. This is represented by the negative value of the cosine of wetting angle. Since the produced hydrogen is not consumed, the steady-state regime is established.

A different behavior can be observed when the hydrogen output is opened (see Figure 3b). The hydrogen output was simulated as release of the gas in atmosphere through a specially designed outlet.

Hence, hydrogen flow is proportional to a difference of the pressures in the reaction chamber and atmosphere. Variation of cosine of the wetting angle from 1 to 0 corresponds to the subsequent drop fallings. The water amount in the second chamber decreases due to the chemical reaction and increases when the subsequent drop falls. Hydrogen pressure increases when the fallen drop provoke reaction of the nanopowder oxidation and decreases when the output hydrogen flow is larger than the hydrogen generation velocity. Thus, the pressure oscillations are observed. Oscillations of the hydrogen flow rate are present as well. In general, the hydrogen flow rate can be smoothed by choice of appropriate system parameters.

As follows from figure 3, the cartridge can be switched from a steady state mode to hydrogen release mode and vice versa by opening/locking the hydrogen outlet. It ensures a self-regulating reaction determined by hydrogen consumption by a fuel cell.

5 Experimental measurements

All the experiments described below have been carried out on a working cartridge prototype using the chemical reaction (2) between aluminum nanopowder and alkaline solution. Rubber balloon (100 ml in volume) was used as the first chamber with pressurized air. A glass container (150 ml in volume) with a hard rubber cover was used as the reaction chamber. Small needle was used as an input needle for the liquid oxidizing reagent, and 75 μm needle radius was found to be suitable for production of necessary hydrogen flow. The output needle has a larger diameter to ensure quick hydrogen delivery to a fuel cell. Before starting the experiments with a fuel cell, the reactor chamber, connecting pipes and fuel cell have been cleaned with nitrogen or argon.

Kinetics of the drop fallings with free release of generated hydrogen in atmosphere is shown in Figure 4. The pressure in the reaction chamber was by 1050 Pa above the atmospheric pressure during the experiment. Every point in Figure 4 correlates the total number of the fallen drops and time of each drop falling. A perfect linear fit of the obtained plot can be performed. If the solid reagent (nanopowder) runs out, the frequency of the drop fallings increases in order maintain hydrogen pressure at a constant level: larger amount of water is thus required. The experiment was carried out only for 700 s, but at a larger amount of the reaction compounds, or lower hydrogen consumption, the working time can be extended.
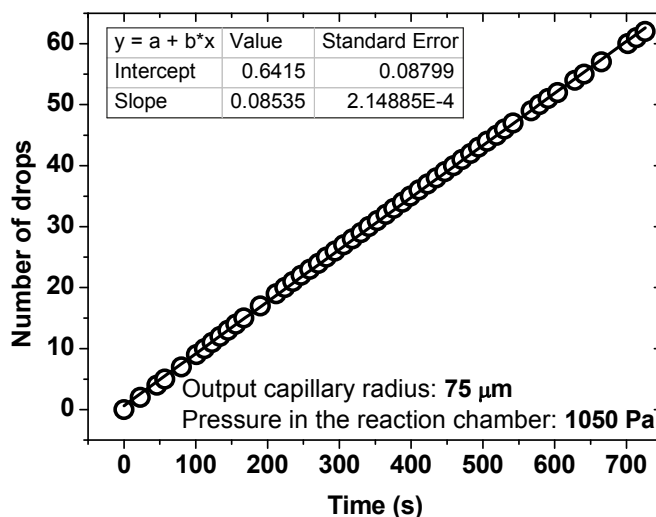

y = a + b*x	Value	Standard Error
Intercept	0.6415	0.08799
Slope	0.08535	2.14885E-4

Output capillary radius: **75 μm**
Pressure in the reaction chamber: **1050 Pa**

Figure 4 – Number of the fallen drops of the liquid reagent as function of time

Electrical characteristics of the used fuel cell are presented in Figure 5. Measurements of the fuel cell characteristics were carried out with a commercial high-purity hydrogen generator. Different load resistances were used. Electrical current in the circuit and voltage on the load resistance were measured directly. The fuel cell voltage was calculated taking into account its own internal resistance. Fuel cell voltage decreases with increasing current, that is typical for such kind of

devices [21] at low currents (less than an optimal current). The optimal current (when maximum electrical power can be achieved) for the tested fuel cell was about 3A. During the next experiments with the fuel cell, the current did not exceed 400 mA.
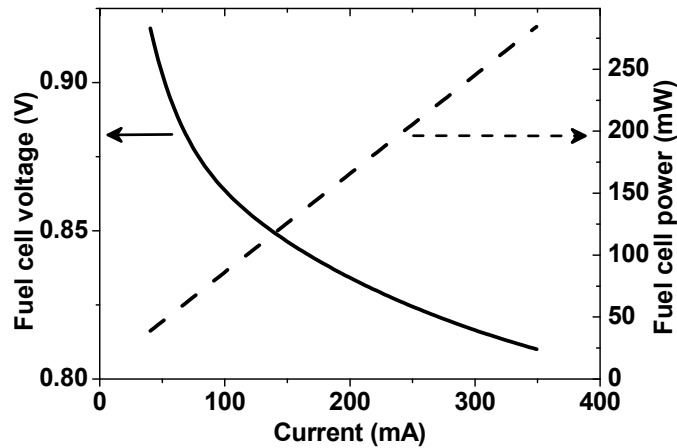

Figure 5 – Electrical characteristics of the used fuel cell

Functioning of the fuel cell supplied by hydrogen produced in our cartridge as function of the load resistance is shown on Figure 6. In this case, in order to ensure a quick delivering of hydrogen to the fuel cell, a thick output needle (250 μm in radius) has been used. The load resistance values were chosen to be: 100, 10, and 1 Ohms. During the measurements, falling of the drops was also observed. The lower the load resistance is, the higher the current is and the more frequent the drop falling is. It means that the fuel cell consumes the hydrogen produced by the chemical reaction in the cartridge. Current and voltage on the load resistance are shown in Figure 6 for different pressures in the chamber with pressurized air: dashed lines correspond to lower pressure, solid lines – to higher pressure. The higher pressure in the first chamber corresponds to higher electric power. By switching load resistance down to 1 Ohm, the higher power of fuel cell is achieved. As a result, higher hydrogen consumption takes place, and more frequent drop falling is observed.
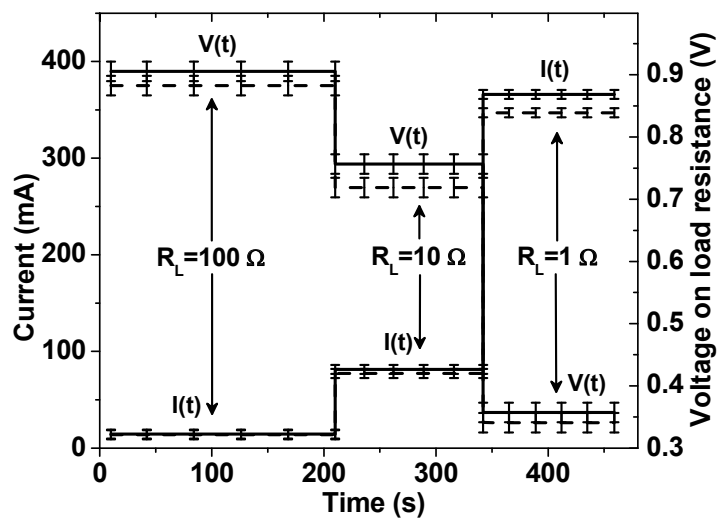

Figure 6 –Variation of the current in the circuit and voltage on the load resistance as function of the resistance value

A. Pastushenko *et al.*

Kinetics of the drop fallings was measured at different load resistances as shown in Figure 7. For each load resistance, the obtained data can be linearly fitted. The fitting line slopes are 0.024, 0.040, and 0.433 s^{-1}, respectively. The relative errors of the fitting do not exceed 10 %. The slope of the curve is proportional to the electric power consumed by the load resistances. By switching from 100 to 50 Ohm the electric power increases about 2 times. In contrast, by switching from 100 Ohm to 1 Ohm the power increases approximately only by 20 times, which corresponds to the I-V characteristic (see Figure 5) of the used fuel cell.

Due to the heat production during the reaction (2), the temperature of the reaction mixture increases. Established temperature depends on the heat exchange with air. Process of the temperature evolution for the chemical reaction with aluminum powder is shown in Figure 8 for the different load resistance. The load resistances were: 100, 10, 5, and 2 Ohms. One can see a strong correlation between the established temperature and the load resistance: the less the load resistance is, the higher the established temperature is and, at the same time, the higher the thermal power is produced.
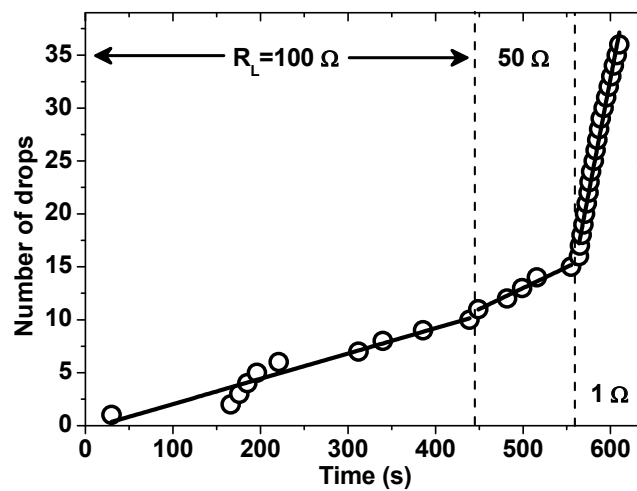

Figure 7 - Number of the fallen drops of the liquid reagent as function of time for different load resistance values
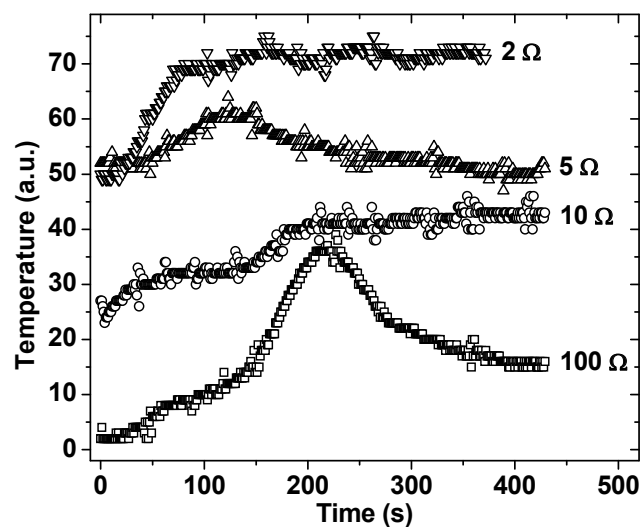

Figure 8 -Time dependent evolution of temperature in the reaction chamber as function of the load resistance

6. Conclusions

In the present work, a device for self-regulated hydrogen production was theoretically designed and experimentally characterized. The device consists of two chambers: the first chamber with pressurized air and liquid reagent, and the second chamber contains solid nanopowder reagent. Porous silicon or aluminum nanopowders can be used as solid reagents. The water with catalyst for porous silicon or alkali for aluminum were used as liquid reagent. The control mechanism was realized by means of a capillary tube connecting the first chamber with the second one. If the pressure difference between the chambers became higher than the capillary pressure (due to consumption of the generated hydrogen), the drop falls from the first chamber and hydrogen evolution leads to a decrease of the pressure difference. If the pressure difference is less than the capillary pressure and hydrogen is not consumed, the system achieve a steady state mode. Experimental results of the performed testing of the device prototype are in excellent agreement with the numerical simulation. The major advantages of the device described in the present article are:

i) working in a drop mode allows delivering of the electrical power for portable electronic devices;

ii) the involved regulation mechanism consumes no electrical power, so that the higher total efficiency can be achieved.

References

1. N.K. Zhevago, E.I. Denisov, V.I. Glebov. Experimental investigation of hydrogen storage in capillary arrays //Int. J. Hydrogen Energy. -2010. –Vol. 35. – P. 169-175.

2. N. Zhevago, E. Denisov. Apparatus for storage and liberation of compressed hydrogen gas in microcylindrical arrays and systems for filling the microcylindrical arrays // US Patent 7,870,878. - 2011.

3. J. Dong, X. Wang, H. Xu, Q. Zhao, J. Li. Hydrogen storage in several microporous zeolites // Int. J. Hydrogen Energy. – 2007. –Vol. 32. –P. 4998-5004.

4. B. Sakintuna, F. Lamari-Darkrim, M. Hirscher. Metal hydride materials for solid hydrogen storage: A review // Int. J. Hydrogen Energy. – 2007. –Vol. 32. –P. 1121-1140.

5. P. Kerrebrock, S. Wayne. Hydrogen generation by hydrolysis of hydrides for undersea vehicle fuel cell energy systems // U.S. Patent 5,372,617. - 1994.

6. K.S. Eom, K.W. Cho, H.S. Kwon. Hydrogen generation from hydrolysis of NH_3BH_3 by an electroplated Co–P catalyst // Int. J. Hydrogen Energy. -2010. –Vol. 35. – P. 181-186.

7. J. Macanás, L. Soler, A.M. Candela, M. Muñoz, J. Casado. Hydrogen generation by aluminum corrosion in aqueous alkaline solutions of inorganic promoters: The Al hydrox process // Energy. -2011. –Vol. 35. – P. 2493-2501.

8. S. Litvinenko, S. Alekseev, V. Lysenko, A. Venturello, F. Geobaldo, L. Gulina, G. Kuznetsov, V. Tolstoy, V. Skryshevsky, E. Garrone, D. Barbier. Hydrogen production from nano-porous Si powder formed by stain etching // Int. J. Hydrogen Energy. -2010. –Vol. 35. –P. 6773-6778.

9. V. Lysenko, F. Bidault, S. Alekseev, V. Zaitsev, D. Barbier, Ch. Turpin, F. Geobaldo, P. Rivolo, E. Garrone. Study of porous silicon nanostructures as hydrogen reservoirs // J. Phys. Chem. B. -2005. –Vol. 109. – P. 19711.

10. Ch. Zhan, P.K. Chu, D. Ren, Y. Xin, K. Huo, Y. Zou, N.K. Huang. Release of hydrogen during transformation from porous silicon to silicon oxide at normal temperature // Int. J. Hydrogen Energy. -2011. –Vol. 36. –P. 4513.

11. A.I. Manilov, S.A. Alekseev, V.A. Skryshevsky, S.V. Litvinenko, G.V. Kuznetsov, V. Lysenko. Influence of palladium particles impregnation on hydrogen behavior in meso-porous silicon // J. Alloys Compd. -2010. –Vol. 492. – P. 466.

12. A.I. Manilov, S.V. Litvinenko, S.A. Alekseev, G.V. Kuznetsov, V.A. Skryshevsky. Use of powders and composites based on porous and crystalline silicon in the hydrogen power industry // Ukr. J. Phys. – 2010. –Vol. 55. – P. 928.

13. D. Buttard, G. Dolino, C. Faivre. Porous silicon strain during in situ ultrahigh vacuum thermal annealing // J. Appl. Phys. – 1999. –Vol.85. –P. 7105.

14. E. Vázquez and J. Tagüeña-Martínez, Surface relaxation effects on the properties of porous silicon, J. Appl. Phys. -2002. –Vol. 91. – P. 3085.

15. D. Kovalev, V. Yu. Timoshenko, N. Künzner, E. Gross, F. Koch. Strong explosive interaction of hydrogenated porous silicon with oxygen at cryogenic temperatures // Phys. Rev. Lett. – 2001. – Vol. 87. –P. 068301.

16. F. V. Miculec, J.D. Kirtland, M.J. Sailor. Explosive nanocrystalline porous silicon and its use in atomic emission spectroscopy // Adv. Mater. -2002. –Vol.14. – P. 38.

17. P. Rivolo, F. Geobaldo, M. Rocchia, G. Amato, A. M. Rossi, E. Garrone. Joint FTIR and TPD study of hydrogen desorption from p+□type porous silicon // Phys. Stat. Sol. A. -2003. –Vol. 197. –P. 217.

18. T. Nychyporuk, V. Lysenko, D.Barbier. Fractal nature of porous silicon nanocrystallites // Phys. Rev. B. -2005. –Vol. 71. –P. 115402.

19. P. Kale, A.C. Gangal, R. Edla, P. Sharma. Investigation of hydrogen storage behavior of silicon nanoparticles // Int. J. Hydrogen Energy. -2012. –Vol. 37. –P. 3741.

20. S. Moghaddam, E. Pengwang, R.I. Masel, M.A. Shannon. A self-regulating hydrogen generator for micro fuel cells // J. Power Sources. -2008.-Vol. 185. –P. 445-450.

21. B. Tazi, O. Savadogo. Parameters of PEM fuel-cells based on new membranes fabricated from Nafion®, silicotungstic acid and thiophene // Electrochim. Acta. -2000. –Vol. 45. –P. 4329-4339.

22. B.J. Kirby. Micro- and nanoscale fluid mechanics: transport in microfluidic devices, Cambridge U.P., New York, 2010.